

Few-Shot Electronic Health Record Coding through Graph Contrastive Learning

Shanshan Wang, Pengjie Ren, Zhumin Chen*, Zhaochun Ren, Huasheng Liang, Qiang Yan, Evangelos Kanoulas, and Maarten de Rijke

Abstract—Electronic health record (EHR) coding is the task of assigning ICD codes to each EHR. Most previous studies either only focus on the frequent ICD codes or treat rare and frequent ICD codes in the same way. These methods perform well on frequent ICD codes but due to the extremely unbalanced distribution of ICD codes, the performance on rare ones is far from satisfactory. We seek to improve the performance for both frequent and rare ICD codes by using a contrastive graph-based EHR coding framework, CoGraph, which re-casts EHR coding as a few-shot learning task. First, we construct a *heterogeneous EHR word-entity* (HEWE) graph for each EHR, where the words and entities extracted from an EHR serve as nodes and the relations between them serve as edges. Then, CoGraph learns similarities and dissimilarities between HEWE graphs from different ICD codes so that information can be transferred among them. In a few-shot learning scenario, the model only has access to frequent ICD codes during training, which might force it to encode features that are useful for frequent ICD codes only. To mitigate this risk, CoGraph devise two graph contrastive learning schemes, GSCL and GECL, that exploit the HEWE graph structures so as to encode transferable features. GSCL utilizes the intra-correlation of different sub-graphs sampled from HEWE graphs while GECL exploits the inter-correlation among HEWE graphs at different clinical stages.

Experiments on the MIMIC-III benchmark dataset show that CoGraph significantly outperforms state-of-the-art methods on EHR coding, not only on frequent ICD codes, but also on rare codes, in terms of several evaluation indicators. On frequent ICD codes, GSCL and GECL improve the classification accuracy and F1 by 1.31% and 0.61%, respectively, and on rare ICD codes CoGraph has more obvious improvements by 2.12% and 2.95%.

Index Terms—Electronic health record (EHR) coding, few-shot learning, graph contrastive learning.



1 INTRODUCTION

THE *International Classification of Diseases* (ICD)¹ is a globally used diagnostic tool for epidemiology, health management and clinical purposes that is commonly used in clinical practice to facilitate billing activities, epidemiology assessment and so on [5, 1]. Automatic *electronic health record* (EHR) coding is the process of assigning ICD codes to EHRs. The task is increasingly attracting attention as manual EHR coding is time-consuming and error-prone.

Automatic EHR coding is non-trivial because the ICD code space is large and their distribution is extremely imbalanced. For instance, 4,065 out of 6,879 ICD codes appear less than 10 times in the MIMIC-III dataset [17]. Frequent ICD codes are generally easier to predict using machine-learning based methods than less frequent ones. Due to a lack of training samples, the performance of predicting rare ICD codes is far from satisfactory. Most

automated EHR coding methods focus on the top 50 or 100 most frequent ICD codes and ignore less frequent ICD codes [e.g., 55, 14, 50]. Such methods are not very practical as the rare ICD codes form a large fraction of the total number. In contrast, in some studies [e.g., 27, 2], rare ICD codes are treated in the same way as frequent ones. However, such methods perform well only for frequent ICD codes. A few studies aim to improve the prediction performance on rare ICD codes through data augmentation [e.g., 60, 44]. They enrich the information of rare ICD codes by introducing external knowledge or synthesizing data. Hence, they rely heavily on the quality of external knowledge sources or synthetic data. However, such knowledge or synthetic data is generally difficult to obtain.

We propose an alternative, graph based few-shot EHR coding approach, called CoGraph (**C**ontrastive **G**raph **C**oding), to improve the EHR coding performance for both *frequent* and *rare* ICD codes. First, we construct a *heterogeneous EHR word-entity* (HEWE) graph for each EHR, where words and entities extracted from an EHR serve as nodes. The relations (i.e., containing relation between EHR and words, co-occurrence relation of words, mention relation of entity in Wikipedia) serve as edges. Then, for each individual HEWE graph, the ICD prediction task for each ICD code is treated as a meta-task where the probability represents the likelihood that the ICD will be assigned to one HEWE graph. By switching

* Corresponding author.

- Shanshan Wang, Pengjie Ren, Zhumin Chen and Zhaochun Ren are with Shandong University, Qingdao, China.
E-mails: wangshanshan5678@gmail.com, jay.ren@outlook.com, chen-zhumin@sdu.edu.cn and zhaochun.ren@sdu.edu.cn.
- Huasheng Liang and Qiang Yan are with WeChat, Tencent, Guangzhou, China.
E-mails: watsonliang@tencent.com and rolanyan@tencent.com.
- Evangelos Kanoulas and Maarten de Rijke are with University of Amsterdam, Amsterdam, The Netherlands.
E-mails: e.kanoulas@uva.nl and m.derijke@uva.nl.

1. <https://www.cdc.gov/nchs/icd/icd9cm.htm>

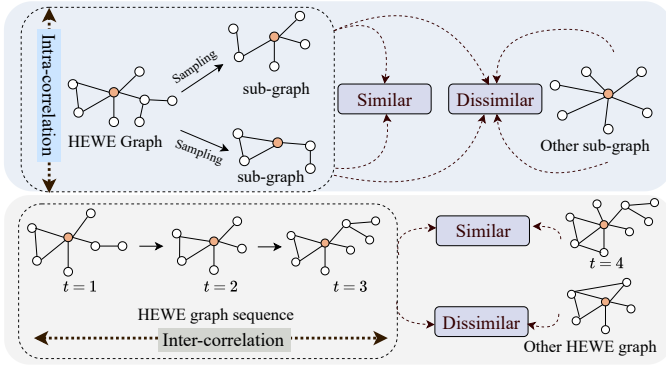


Fig. 1: (Top): A diagram of the contrast between the sampled sub-graphs from initial HEWE graphs. (Bottom): A diagram of the contrast between a historical HEWE graph sequence and future graph at different clinical stages. The orange node is a virtual EHR node. t is the t -th HEWE graph of the same patient.

between different meta-tasks constructed from frequent ICD codes during training, CoGraph allows us to extract transferable information across different ICD codes. As a result, CoGraph cannot only improve the prediction of frequent ICD codes; it can also boost the performance of rare ICD codes with just a small number of labeled HEWE graphs, by using prior information transferred from non-overlapping frequent ICDs that have sufficient HEWE graphs.

This is not enough. In a few-shot classification scenario, learning methods only have access to instances belonging to frequent classes. Without correction this may push a learning method to only encode features that are useful for distinguishing frequent ICDs, while discarding those that might be critical for rare ICDs [35, 40]. To mitigate this risk, CoGraph leverages self-supervised representation learning techniques [57, 4] for HEWE graphs by limiting the dependence of the framework on the ICD codes. To this end, we propose two graph contrastive learning schemes to exploit information available from the HEWE graph structure itself to learn better transferable features, namely *graph sampling contrastive learning* (GSCL) and *graph evolution contrastive learning* (GECL).

GSCL explores the *intra*-correlation of sub-graphs sampled from the HEWE graphs, as illustrated in Fig. 1 (top). The intuition behind this is that each sampled sub-graph is a part of the whole HEWE graph, hence the sub-graphs are contextually relevant to each other if they come from the same HEWE graph. The representation of the sub-graph is thus encouraged to capture the shared structural information inherited from the HEWE graph. In contrast, GECL exploits the *inter*-correlation among HEWE graphs at different clinical stages, as illustrated in Fig. 1 (bottom). The intuition behind it is that HEWE graphs from the same patient can be expressed as an evolving graph sequence and display temporal coherence and consistency. The history such a HEWE graph sequence together with the future HEWE graph are considered as similar pairs while the history with another HEWE graph picked from other sequences are

considered to be dissimilar ones. Hence, by learning invariant, slowly changing features in an evolutionary HEWE graph sequence, a model will learn to reserve more important features in the HEWE graphs.

Because the two graph contrastive learning schemes, GSCL and GECL, do not rely on the ICD labels for each EHR as they define positive and negative samples by contrast, they can help encode unbiased transferable features. Moreover, by extending the size and variety of training data in this manner, we expect CoGraph to learn stronger HEWE graph features and achieve performance gains. To verify the effectiveness of CoGraph and compare GSCL and GECL schemes, we conduct experiments on the MIMIC-III benchmark dataset [17]. The experimental results demonstrate that CoGraph significantly outperforms state-of-the-art methods by a large margin, and that two graph contrastive learning schemes can further improve model’s performance.

To sum up, the contributions of this work are as follows:

- We introduce CoGraph, a graph-based few-shot EHR coding framework for boosting the prediction capability on both frequent and rare ICD codes.
- We devise *graph sampling contrastive learning* and *graph evolution contrastive learning* schemes by exploring the intra-correlation of each HEWE graph and the inter-correlation among sequential HEWE graphs at different clinical stages.
- We carry out extensive experiments on the MIMIC-III benchmark dataset to verify and analyze the effectiveness of CoGraph.

2 RELATED WORK

Related work comes in three directions: 1) automatic EHR coding, 2) few-shot learning, and 3) graph contrastive learning.

2.1 Automatic EHR coding

In recent years, the automatic EHR coding task has been studied extensively. Most EHR coding methods focus on (some) frequent ICD codes and ignore rare ICD codes. Huang et al. [14] perform two data preprocessing methods; the first only considers the top 10 and top 50 common ICD codes; the second groups ICD codes into categories based on their hierarchical nature; they extract features from EHRs and train an ICD prediction model using deep learning. Wang et al. [50] use the hierarchical nature of ICD codes and divide them into 19 categories at the upper level for the most general classification and 129 categories at the lower level for more specific classifications. Xu et al. [55] develop an ensemble-based approach that integrates three modality-specific models to predict 32 selected ICD codes. Shi et al. [36] propose a soft-attention mechanism that learns to allocate attention strengths on multiple diagnosis descriptions when assigning the 50 most frequent ICD codes.

As we pointed out in the introduction, the frequency distribution of ICD codes is imbalanced; rare ICD codes

account for a large proportion. Some EHR coding methods treat rare ICD and frequent ICD codes equally. Mullenbach et al. [27] aggregate information across a EHR by using a convolutional neural network and use an attention mechanism to select the most relevant segments for each ICD code. Similarly, Baumel et al. [2] present a Hierarchical Attention-bidirectional Gated Recurrent Unit (HA-GRU), a hierarchical approach to tag an EHR by identifying the sentences relevant for each ICD code. Wang et al. [52] propose a coarse-to-fine ICD path generation framework to generate ICD codes from lower levels to higher levels in the ICD hierarchy.

Very few publications pay specific attention to rare ICD codes and make an effort to improve the prediction performance on rare ICD codes. Zhang et al. [60] propose a method that retrieves PubMed articles with ICD descriptions to enrich the training data of rare ICD codes; they extract 500 features from EHRs and use several classic classifiers, such as SVM and LR, to predict ICD codes for each EHR. Teng et al. [44] use the ICD description as a query to match content pages in Freebase; the entities extracted from the matched Freebase pages form a knowledge graph, and a better ICD representation is learned based on this knowledge graph; finally, they predict ICD codes by matching the EHR representation with each ICD representation.

Unlike most of the EHR coding methods listed above, we aim to improve the prediction of *frequent* and *rare* ICD codes at the same time. Compared with existing methods for improving *frequent* and *rare* ICD code prediction, CoGraph, the graph-based few-shot framework that we propose, can inject external knowledge into the HEWE Graphs to enrich EHR information. Moreover, it transfers internal knowledge from predicting frequent ICDs to rare ICD codes in order to improve the prediction performance on rare ICD codes.

2.2 Few-shot learning

Few-shot learning (FSL) aims to transfer knowledge from frequent classes that generalizes well to classes where only a few samples are available [23, 34]. Existing FSL methods can be divided into optimization-based methods and metric-based methods.

Optimization-based methods achieve FSL by improving the optimization processes, e.g., model initialization, parameter updating. E.g., the LSTM-based meta-learner proposed by Ravi and Larochelle learns the exact optimization algorithm used to train another neural network classifiers in the few-shot regime. Finn et al. [7] learns better parameter initialization that is suitable for different FSL tasks and is compatible with any model trained with gradient descent. Li et al. [22] present Meta-SGD that learns the parameter initialization, gradient update direction, and learning rate with a one step update. Mishra et al. [26] combine temporal convolution and soft attention to learn an optimal learning strategy.

Metric-based methods are based on nearest neighbor-based methods and kernel density estimation [10], which

learn an effective metric and similarity function. Matching networks [49] make predictions by comparing the input example with a few-shot labeled support set by the cosine distance, and weighted the labels of support set to get the prediction label. Snell et al. [38] propose prototypical networks that learn a metric space where classification can be performed by computing squared Euclidean distances to prototype representations of each class. Unlike fixed metric measures, relation networks learn a deep distance metric to compare the query with given examples [42].

CoGraph is a metric-based method. The differences between the work listed above and our work are least two-fold. First, we are the first to propose a few-shot EHR coding method based on HEWE graphs. Second, we design two graph contrastive learning schemes to alleviate the issue that metric-based methods might fail to encode features that are critical for rare ICD codes.

2.3 Graph contrastive learning

Contrastive learning is a learning paradigm to learn distinctiveness, i.e., what makes two objects similar or different. It has received interest due to its success in self-supervised representation learning in natural language processing [25, 9] and computer vision [53, 45, 12]. Graph contrastive learning extends the paradigm to representation learning on graphs. Peng et al. [29] learn node representations by randomly selecting pairs of nodes in a graph and training a neural network to predict the contextual position of one node relative to others. Velickovic et al. [48] train a node encoder that maximizes the mutual information between a node representation and the pooled global representation. Zeng and Xie [59] define four basic graph alteration operations including edge deletion, edge insertion, node deletion, and node insertion on original graphs to create augmented graphs; they then devise a contrastive learning method to distinguish whether two augmented graphs are from the same original graph. Qiu et al. [32] introduce graph contrastive coding (GCC), which defines the pre-training task as subgraph instance discrimination and leverages contrastive learning to learn structural representations; their work is the most similar to the graph sampling contrastive learning (GSCL) that we propose in this work, but GCC learns graph structure by determining whether two sub-graphs originate from the same source graph, while GSCL captures the intra-correlation in the HEWE graph structure by matching the embeddings of two sub-graphs. In addition, GSCL is not independent, and it needs to combine with GECL to pre-train the graph encoder. GECL is able to capture invariant, slowly changing features by mining evolving HEWE graph sequences.

3 PRELIMINARIES

3.1 Graph construction

For each EHR, we build a HEWE graph that can be represented as a tuple $G = (V, E, X)$, where V denotes

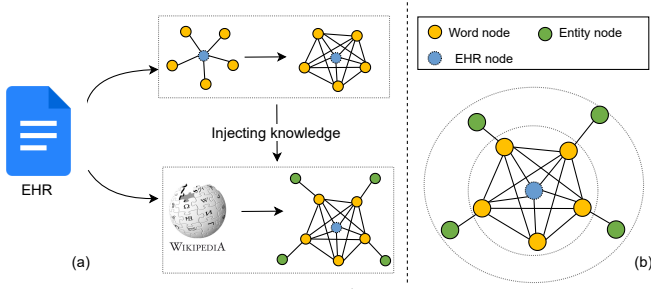


Fig. 2: HEWE graph construction.

the set of nodes v_1, v_2, \dots, v_n and E denotes the set of edges e_1, e_2, \dots, e_m . A HEWE graph contains three kinds of nodes: 1) a virtual EHR node, 2) word nodes, and 3) entity nodes. The process for constructing the HEWE graph is illustrated in Fig. 2. First of all, we only preserve high-frequency words in one EHR and regard them as word nodes [51]. An edge between the EHR node and a word node is established if the word appears in the corresponding EHR. Then we use a fixed-size sliding window on each EHR to gather co-occurrence words, to utilize global word co-occurrence information. If two words appear in the same sliding window, we will create an edge between the two word nodes. Finally, we inject the knowledge from Wikipedia² into the HEWE graph to enrich the EHR information. Specifically, we use each word as a query to search the Wikipedia and consider the most relevant entity as the entity node. Similarly, an edge is established between the word and the entity nodes. All the edge weights are set to 1.

Moreover, each node v_i is associated with a feature vector $\mathbf{x}_i \in R^{1 \times d}$ and $\mathbf{X} = [x_1; x_2; \dots; x_n] \in R^{n \times d}$ denotes all the node features. d is the dimension of feature vector and n is the number of all nodes in a HEWE graph. Thus, a HEWE graph can be represented as a pair $G = (\mathbf{A}, \mathbf{X})$, where $\mathbf{A} \in R^{n \times n}$ is an adjacency matrix representing the network structure. Specifically, $A_{i,j} = 1$ indicates that there is an edge between node v_i and node v_j ; otherwise, $A_{i,j} = 0$.

3.2 Problem statement

Following the common setting in FSL, at each episode in the meta-training, the model takes C ICD codes and selects K HEWE graphs per ICD code to constitute the support set S , this problem is also taken as C -way K -shot HEWE graph classification problem. Formally, given a query HEWE graph q and its few-shot support HEWE graphs S , the task is to design an EHR coding model that predicts appropriate ICD code for the query HEWE graph q . In essence, the objective of this problem is to learn a meta-classifier that can adapt to new ICD classification with only a few labeled HEWE graphs. Therefore, how to extract transferable meta-knowledge from training ICD codes and transfer the knowledge to testing ICD codes is the key for solving the EHR coding problem.

4 METHOD

4.1 Overview

We elaborate the proposed CoGraph whose framework is illustrated in Figure 3. CoGraph consists of two stages: a pre-training stage and a few-shot learning stage.

In the pre-training stage, we pre-train a high-quality graph encoder that is used to initialize the graph encoder in the few-shot learning stage. The pre-training stage contains two schemes: graph sampling contrastive learning (GSCL) and graph evolution contrastive learning (GECL). GSCL and GECL can train a better graph encoder by exploiting graph structure information at the intra-graph level and inter-graph level, respectively. For the HEWE graph sequence of a patient, GSCL captures the intra-correlations of graph structure among sampled sub-graphs by intra-graph contrastive learning. At the inter-graph level, GECL can force the graph encoder to learn the correlations between HEWE graphs at different clinical stages by the inter-graph contrastive learning.

The few-shot learning stage is used to predict the most probable ICD code for each query HEWE graph. Specifically, as shown in Figure 3, the support set is composed of several HEWE graphs sampled from three different ICD codes, i.e., c_1, c_2, c_3 , respectively. First, the query graph and support graphs from the support set are fed into the pre-trained graph encoder to get the representation of each graph. Second, the prototype calculation module is used to calculate the prototype of each ICD code, denoted as $\mathbf{p}_{c_1}, \mathbf{p}_{c_2}$, and \mathbf{p}_{c_3} . Third, CoGraph calculates the similarity between the query graph \mathbf{g}_q and each ICD prototype \mathbf{p}_{c_i} ($i = 1, 2, 3$). The ICD prototype with the highest similarity score (c_3 in Figure 3, for instance) is the predicted ICD for the query graph.

4.2 Graph sampling contrastive learning

In order to capture the intra-graph structure and overcome the dependence on ICD codes, we introduce the concept of graph sampling. Formally, given a HEWE graph, $G = (\mathbf{A}, \mathbf{X})$, graph sampling is a sampling strategy on nodes and relations of G to produce a random sub-graph $\tilde{G} = (\tilde{\mathbf{A}}, \tilde{\mathbf{X}})$. There are various sampling strategies for graph data, such as feature corruption and node masking [16, 15, 61]. We adopt a node masking-based sub-graph sampling strategy to produce sub-graphs for its simplicity and effectiveness. Specifically, we regard the EHR node in the HEWE graph as the central node and randomly mask half of neighbor nodes of the central node. Correspondingly, the edges associated with these masked nodes are set to 0. The graphs obtained by node masking are called the *sub-graphs*. We perform two times of node masking operations randomly to produce two sub-graphs for each HEWE graph.

Given one sub-graph \tilde{G}_i , a HEWE graph encoder is used to encode them to obtain the latent representations matrices $\tilde{\mathbf{H}}_i$. The corresponding calculation formula can be denoted as:

$$\tilde{\mathbf{H}}_i = \text{encoder}(\tilde{\mathbf{X}}_i, \tilde{\mathbf{A}}_i), \quad (1)$$

2. https://en.wikipedia.org/wiki/Main_Page

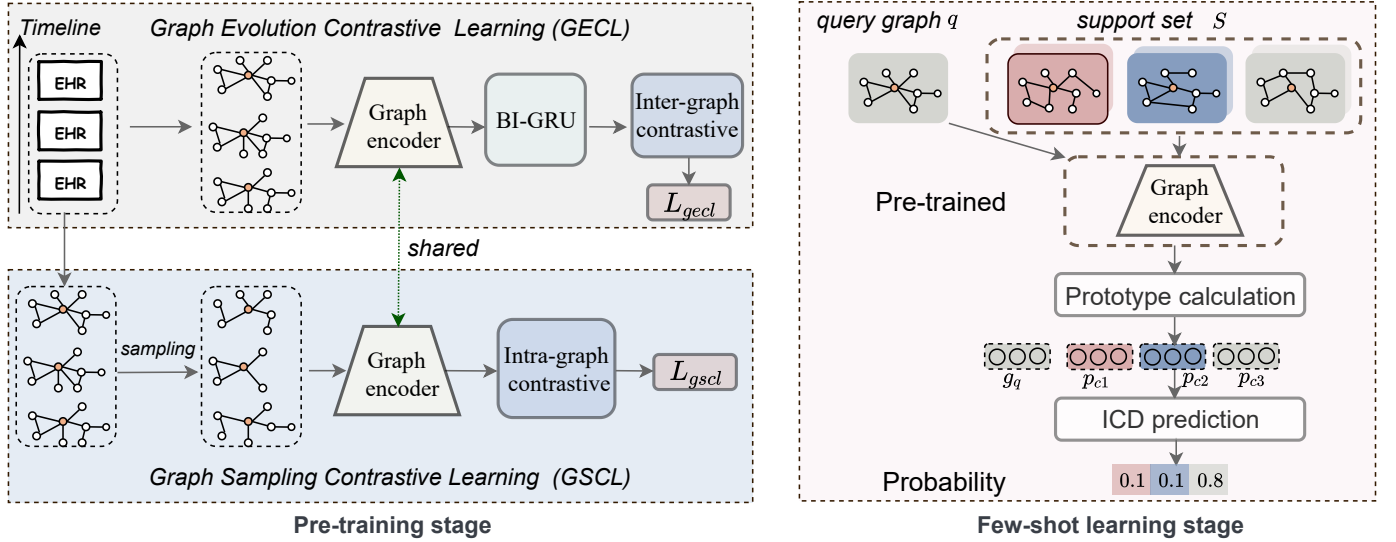


Fig. 3: A schematic diagram of proposed CoGraph model.

where $\tilde{\mathbf{X}}_i$ and $\tilde{\mathbf{A}}_i$ represent node feature vector and adjacency matrix of sub-graph \tilde{G}_i sampled from HEWE graph G_i .

Here we adopt a two layers graph convolutional network (GCN) [20], a flexible node embedding architecture, as the graph encoder. More specifically, the two layers GCN we use can be defined as:

$$\begin{aligned} \bar{\mathbf{A}}_i &= \mathbf{D}^{-\frac{1}{2}} \check{\mathbf{A}}_i \mathbf{D}^{-\frac{1}{2}}, \\ \tilde{\mathbf{L}}_i &= \text{ReLU}(\bar{\mathbf{A}}_i (\tilde{\mathbf{X}}_i \mathbf{W}_0 + \mathbf{b}_0)), \\ \tilde{\mathbf{H}}_i &= \text{ReLU}(\bar{\mathbf{A}}_i (\tilde{\mathbf{L}}_i \mathbf{W}_1 + \mathbf{b}_1)). \end{aligned} \quad (2)$$

Here, $\check{\mathbf{A}}_i = \tilde{\mathbf{A}}_i + \mathbf{I}_N$ is the adjacency matrix of the sub-graph \tilde{G}_i with added self-connections. \mathbf{I}_N is the identity matrix and $D_{i,i} = \sum_j \check{A}_{i,j}$. $\tilde{\mathbf{X}}_i$ is the initial feature matrix of all nodes in the sub-graph \tilde{G}_i ; $\tilde{\mathbf{L}}_i$ and $\tilde{\mathbf{H}}_i$ are the node representations at different layers in GCN; \mathbf{W}_0 and \mathbf{W}_1 are parameter matrices; \mathbf{b}_0 and \mathbf{b}_1 are biases.

The central node embedding $\tilde{\mathbf{g}}_i$ in sub-graph \tilde{G}_i is picked from the latent representation matrix $\tilde{\mathbf{H}}_i$:

$$\tilde{\mathbf{g}}_i = \mathcal{P}(\tilde{\mathbf{H}}_i), \quad (3)$$

where \mathcal{P} denotes the operation of picking out the central EHR node embedding from embedding matrix. Since $\tilde{\mathbf{g}}_i$ denotes the central EHR node in the sub-graph \tilde{G}_i , we can use it as the global representation of sub-graph \tilde{G}_i .

We randomly sample a mini-batch of N HEWE graphs and produce $2N$ sub-graphs since we sample two times for each HEWE graph. Then we define the GSCL task on pairs of sampled sub-graphs derived from the mini-batch. For a sub-graph sampled from a specific central EHR node, our approach for learning the graph encoder relies on contrasting its real sub-graph instances with fake ones. Specifically, we regard the pair of two sub-graphs sampled from the same HEWE graph as a positive pair. We do not sample negative examples explicitly. Instead, given a positive sub-graph pair, similar to [3],

we treat the other $2(N-1)$ sub-graph pairs within a mini-batch as negative samples.

The loss function we used is termed as the *NT-Xent* (the normalized temperature-scaled cross entropy loss) and has been used widely in previous work [39, 53, 46]. Let $\text{sim}(\mathbf{u}, \mathbf{v}) = \mathbf{u}^T \mathbf{v} / \|\mathbf{u}\| \|\mathbf{v}\|$ denotes the dot product between ℓ_2 normalized \mathbf{u} and \mathbf{v} (i.e., cosine similarity). Then the *NT-Xent* loss for a positive sub-graph pair of (i, j) is defined as:

$$l(i, j) = -\log \frac{\exp(\text{sim}(\mathbf{g}_i, \mathbf{g}_j) / \tau)}{\sum_{k=1}^{2N} \mathbb{1}_{[k \neq i]} \exp(\text{sim}(\mathbf{z}_i, \mathbf{z}_k) / \tau)}, \quad (4)$$

where $\mathbb{1}_{[k \neq i]} \in \{0, 1\}$ is an indicator function evaluating to 1 if $k \neq i$ and τ denotes a temperature parameter. In the experiment, we set τ to 0.5. The final loss is computed across all positive pairs, both (i, j) and (j, i) , in a mini-batch. Using the pairwise similarities for each positive pair of sub-graphs, the loss function of GSCL scheme is aggregated with the following formula:

$$L_{gscl} = \frac{1}{2N} \sum_k^N [l(2k-1, 2k) + l(2k, 2k-1)], \quad (5)$$

4.3 Graph evolution contrastive learning

An important intuition that we build is that the past states of a patient contain relevant information about their future states. Correspondingly, by contrastive learning of past HEWE graphs and future HEWE graph of each patient, the relevant information between the graphs in the sequence can be captured. Formally, given a patient o , their T EHRs form an HEWE graph sequence according to the recording time. That is, $o = [G_1, G_2, \dots, G_t, \dots, G_T]$, where G_t represents the t -th HEWE graph. Graph evolution is a scheme to learn trends from a history of HEWE graphs to predict a future graph. More specifically, given the historical sequence $[G_1, G_2, \dots, G_{T-1}]$, we aim to predict graph G_T at the latest time.

A bidirectional gate recurrent unit (BI-GRU) network [58] is adopted to model the HEWE graph sequence; it is composed of a forward gated recurrent unit (GRU) unit and a backward GRU unit. The hidden layer output of the forward GRU unit is denoted as \vec{h}_t and the hidden layer output of the backward GRU unit is denoted as \overleftarrow{h}_t . The hidden output of a BI-GRU at time t is spliced through the hidden layer output of forward GRU unit and backward GRU unit, as shown in Eq. 6:

$$\begin{aligned} \vec{h}_t &= \text{GRU}(g_t, \overrightarrow{h_{t-1}}) \\ \overleftarrow{h}_t &= \text{GRU}(g_t, \overleftarrow{h_{t-1}}) \\ \mathbf{h}_t &= [\vec{h}_t, \overleftarrow{h}_t], \end{aligned} \quad (6)$$

where \mathbf{h}_{t-1} is the hidden vector at timestamp $t-1$; g_t is the representation of t -th HEWE graph. We use the graph encoder shared with GSCL to obtain the representation g_t of t -th HEWE graph:

$$\begin{aligned} \mathbf{H}_t &= \text{encoder}(\mathbf{X}_t, \mathbf{A}_t), \\ g_t &= \mathcal{P}(\mathbf{H}_t), \end{aligned} \quad (7)$$

where \mathbf{X}_t denotes node features and \mathbf{A}_t denotes the adjacency matrix in the t -th HEWE graph. We use \mathbf{h}_{T-1} at timestamp $T-1$ as the context representation that forms a summary of past HEWE graph sequence.

Similar to GSCL, we randomly sample a mini-batch of N HEWE graph sequences and then define the GECL task on $2N$ samples derived from the mini-batch. For a HEWE graph sequence, our approach for learning the graph encoder relies on contrasting its real coherent sequence with fake ones. Specifically, the context representation \mathbf{h}_{T-1} and future graph g_T then form a *positive pair*, while replacing the future graph g_T with g_T^* from other HEWE graph sequences will generate *negative pairs*.

Given a pair (\mathbf{h}_{T-1}, g_T) , a powerful mechanism to incorporate the interaction between them is via bilinear pooling [8]. This is essentially an outer product and results in a matrix $\mathbf{Z} \in \mathbb{R}^{d \times d}$:

$$\mathbf{Z} = \mathbf{h}_{T-1} \otimes g_T = \mathbf{h}_{T-1} \times g_T^T, \quad (8)$$

where \otimes denotes the outer product operation of two embeddings. This is followed by a reshaping of the matrix \mathbf{Z} into $\mathbf{z} \in \mathbb{R}^{d^2 \times 1}$:

$$\mathbf{z} = \text{reshape}(\mathbf{Z}), \quad (9)$$

which, in turn, is followed by a linear projection of the result to obtain the output of the interaction u :

$$u = \mathbf{W}_u \times \mathbf{z}, \quad (10)$$

where the \mathbf{W}_u is a learned transformation matrix. The objective of GECL is to predict whether the candidate graph g_T is a correct future graph for the patient. We use the binary cross-entropy loss for model optimization:

$$L_{gecl} = -\frac{1}{N^2} \sum_{i=1}^{N^2} y_i \cdot \log(\sigma(u) + (1-y_i) \cdot \log(1-\sigma(u))), \quad (11)$$

where $\sigma(u) = 1/(1+\exp(-u))$ is the sigmoid function and y_i denotes whether the i -th context-future pair is positive or negative, and M denotes the total number of context-future pairs.

4.4 Co-training

The two graph contrastive learning schemes, i.e., GSCL and GECL, do not depend on ICD labels. So we can easily extend them to learn as well from additional unlabeled HEWE graphs and we can make GSCL and GECL benefit from each other by jointly training:

$$\min_{\theta} (L_{gecl} + \alpha L_{gscl}), \quad (12)$$

where α controls the importance of the GSCL task and θ represents all learnable parameters. In the experiments, we set α to 0.5.

4.5 Graph few-shot EHR coding

4.5.1 Overall architecture of few-shot EHR coding

In the few-shot learning stage, we construct an ‘‘episode’’ to compute gradients and update our model in each training iteration[31]. For the C -way K -shot problem, a training episode is formed by randomly selecting C ICD codes from the C_{train} (frequent ICD codes) and choosing K HEWE graphs per selected ICD to act as the support set $S = \bigcup_{i=1}^C \{G_{c_i, s}, y_{c_i, s}\}_{s=1}^K$. A subset of the remaining examples serves as the query set $Q = \{G_q, y_q\}_{q=1}^L$. Training on each episode is conducted by feeding the support set S to the model and updating its parameters to minimize the loss in the query set Q .

4.5.2 Pre-trained graph encoder

In order to learn an expressive HEWE graph representation for each EHR, we develop a graph encoder to capture the graph structure. The encoder structure is exactly the same as the graph encoder in GSCL and GECL, which is a two-layer GCN. Please refer to Eq. 2 for details.

$$\begin{aligned} \mathbf{H}_{c_i, j} &= \text{encoder}(\mathbf{X}_{c_i, j}, \mathbf{A}_{c_i, j}), \\ g_{c_i, j} &= \mathcal{P}(\mathbf{H}_{c_i, j}), \end{aligned} \quad (13)$$

where $g_{c_i, j}$ represents the j -th HEWE graph and it belongs to ICD c_i in the support set S ; $\mathbf{X}_{c_i, j}$ and $\mathbf{A}_{c_i, j}$ represent the node features and adjacency matrix corresponding to this HEWE graph, respectively.

We use GSCL and GECL as tasks to pre-train a HEWE graph encoder and use it to initialize the graph encoder in the few-shot EHR learning stage.

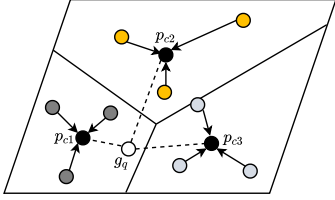


Fig. 4: Prototypical Network for few-shot learning

4.5.3 Prototype calculation

We follow the idea of prototypical networks [38], which encourages HEWE graphs in the support set S_{c_i} to cluster around a specific prototype. The schematic diagram of the prototypical network is illustrated in Fig 4. In this figure, p_{c_1} , p_{c_2} and p_{c_3} denote the prototype representation for ICD code c_1 , c_2 and c_3 , respectively. Formally, the prototype representation of ICD c_i can be computed by:

$$p_{c_i} = P_{roto}(\{g_{c_i,j} | \forall j \in S_{c_i}\}), \quad (14)$$

where S_{c_i} denotes the set of labeled HEWE graphs from ICD code c_i and P_{roto} is the prototype computation function; $g_{c_i,j}$ is the j -th HEWE graph representation for the ICD c_i . The prototype representation p_{c_i} of the ICD c_i is computed by taking the average of all embedded HEWE graphs belonging to the ICD c_i :

$$p_{c_i} = \frac{1}{|S_{c_i}|} \sum_{j=1}^{|S_{c_i}|} g_{c_i,j} \quad (15)$$

4.5.4 ICD prediction

The learned prototypes define a ICD predictor for each query HEWE graph g_q . More specifically, it can assign a probability over ICD code c_i based on the matching score between the query HEWE graph g_q and each ICD prototype p_{c_i} . Specifically, we model this matching relationship as follows:

$$p(c_i | g_q) = \sigma(\mathbf{W}_c(g_q \parallel p_{c_i})), \quad (16)$$

where \parallel denotes the concatenation operation, and \mathbf{W}_c is the weight matrix; g_q is the query HEWE graph representation and p_{c_i} is the prototype representation of class c_i ; $p(c_i | g_q)$ is the probability of the query HEWE graph belonging to ICD c_i .

Under the episodic training framework, the objective of each episode is to minimize the classification loss between the predictions of the query set and the ground-truth. Specifically, for each episode, given the support set S and query set $Q = \{G_q, y_q\}_{q=1}^L$, the training objective is to minimize the cross-entropy loss on the C ICD codes:

$$L_{few}(S, Q) = -\frac{1}{C} \sum_{i=1}^C \frac{1}{L} \sum_{q=1}^L y_q \log(p(c_i | g_q)). \quad (17)$$

By minimizing the above loss function, CoGraph is able to learn a generic classifier for the C_{train} ICD codes. After training on a considerable number of episodes, its

Algorithm 1: The training and testing process of CoGraph

- 1 //Training process
 - 2 Jointly train GSCL and GECL by minimizing the loss in Eq.12;
 - 3 Save the parameters of the graph encoder in Eq.1;
 - 4 Initialize the graph encoder in Eq.13 with the parameters saved in line 3;
 - 5 **for each episode iteration do**
 - 6 Randomly select C ICD codes from the C_{train} ;
 - 7 Randomly select K labeled HEWE graphs from each of the C ICDs as support set S ;
 - 8 Randomly select a fraction of the remainder of those C ICD codes' HEWE graphs as query set Q ;
 - 9 Feed S to the model and minimizing the loss in Eq.17;
 - 10 **end**
 - 11 //Testing process
 - 12 **for each episode iteration do**
 - 13 Randomly select C ICD codes from the C_{test} ;
 - 14 Randomly select K labeled HEWE graphs from each of the C ICDs as support set S ;
 - 15 Randomly select a fraction of the remainder of those C ICD codes' HEWE graphs as query set Q ;
 - 16 Calculate the prototypes for C ICD codes with Eq.15;
 - 17 Predict ICD for each HEWE graph in Q with Eq.16.
 - 18 **end**
-

generalization performance will be measured on the test episodes, which contain HEWE graphs sampled from C_{test} (rare ICD codes) instead of C_{train} . For each test episode, we use the predictor produced by CoGraph for the provided support set S to classify each query HEWE graph in Q . The details of training and testing the CoGraph are shown in Algorithm 1. Firstly, the graph encoder is pre-trained by the GECL and GSCL schemes (line 2-3). Next, the EHR coding model is trained using the labelled data (line 4-10). Finally, the CoGraph is tested for each test episode (line 12-18).

5 EXPERIMENTAL SETUP

5.1 Dataset

We conduct experiments on the MIMIC-III dataset³, which is a large, freely-available database comprising de-identified health-related data associated with over forty thousand patients between 2001 and 2012. This is the only benchmark dataset that is commonly used on this task and publicly available [17]. As with previous studies, e.g., [27, 30], we focus on discharge summaries in EHR, which summarize the information about a stay into a

3. The dataset used in this paper is available at <https://mimic.physionet.org/>.

TABLE 1: Statistics of the MIMIC-III dataset.

Statistics	Training set	Test set
# ICD codes	2,033	3,335
avg # of HEWE graphs	284.45	6.43
# of EHR nodes	51,434	14,519
avg # of word nodes	117.89	101.05
avg # of entity nodes	177.11	187.95
avg # of EHR-word edges	118.01	101.23
avg # of word-word edges	3,903.71	3,293.19
avg # of word-entity edges	92.85	101.45

single document. We count the number of occurrences of each ICD code in the MIMIC-III dataset, and ICD codes are selected as training classes if they occur more than 20 times. Among the remaining ICD codes, the number occurrences of ICD codes selected as testing class should be no less than 2 times, and the remaining ICD codes are filtered. It should be noted that there is no overlapping between training ICD and testing ICD codes. Accordingly, these EHRs are divided into training set and test set according to their ICD codes. The one more thing is we randomly divide the training dataset into training and validation sets with a 7:3 ratio during training. Descriptive statistics of the training set and test set are given in Table 1. It can be observed from Table 1 that the number of ICD codes in the test set is more than that in the training set, and the average number of HEWE graphs in the test set is only 6.43, which is much smaller than that in the training set. Again, this indicates that the distribution of the ICD codes is extremely imbalanced, which demonstrates the challenge of this task.

5.2 Baselines

In order to demonstrate the effectiveness of CoGraph, we compare it with several methods, including state-of-the-art models for EHR coding and few-shot learning methods:

- **Multilayer perceptron (MLP)**. We learn a multi-label classification model with a three-layer perceptron to predict the probability of each ICD code.
- **BI-GRU** [62]. This method uses a bidirectional gated recurrent unit to encode EHR and then performs binary classification on each ICD code based on the EHR representation.
- **CAML** and **DR-CAML** [28]. CAML exploits Text-CNN [18] to obtain the representation of each EHR and then uses label-dependent attention to learn the most informative representation for each ICD code, based on which it does binary classification. DR-CAML enhances CAML by adding an ICD description regularization term to the final classification weights.
- **MSATT-KG** [54]. MSATT-KG leverages a convolutional neural network to produce variable n-gram features for clinical notes and incorporates multi-scale feature attention to adaptively select multi-scale features. The multi-scale features are used to perform multi-label classification over all the ICD codes.
- **Matching Network (MatchingNet)** [49]. MatchingNet first gets the representations of support HEWE graphs

and query HEWE graphs, and then computes the similarity of query graph to each support graph. Finally, the ICDs from the support HEWE graphs are weight-blended together accordingly to predict ICD codes.

- **PrototypeNet** and **PrototypeNet-attention** [37]. PrototypeNet computes the distance between query HEWE graph and each ICD prototype. Then it determines the ICD of the query HEWE graph based on the shortest distance. PrototypeNet-attention assigns different weights to each support graph when calculating the prototype representation of each ICD.
- **RelationNet-attention** [43]. RelationNet-attention is the RelationNet with an attention mechanism; it is composed of an embedding module and a relation module. The embedding module produces the representation of the query and support HEWE graphs. Then the relation module compares these embeddings to determine whether they belong to the same ICD.

5.3 Evaluation metrics

A discussion of performance metrics used for EHR coding is beyond the scope of this paper [30, 28, 54]. We select macro-averaged metrics, i.e., ACC, Precision, Recall, F1, because they are calculated by averaging metrics computed per-ICD [11, 13]. ACC refers to the percentage of correctly classified EHRs among the total number of EHRs. In the case of an imbalanced distribution between different ICD codes, accuracy alone is not enough and more appropriate metrics are Precision and Recall. F1 score is the harmonic mean of Precision and Recall, so it is a relatively impartial evaluation metric.

5.4 Implementation details

For CoGraph, the initial embedding dimension of each node is set to 300. We use a two layer GCN to get the embedding representation of each node and the dimensions of W_0 and W_1 (Eq. 2) are set to 100 and 300, respectively. In the pre-training stage of the graph encoder, we use a BI-GRU to model the graph evolution representation, the hidden size of the BI-GRU in Eq. 6 is set to 300, and the value of α in Eq.12 is set to 0.5. We use the Adam optimizer to optimize the parameters of the two graph contrastive learning schemes. The batch size is to 128 and the learning rate is 0.0001. In the few-shot learning stage, the ICD number C in each episode is set to 5. We pick 5 HEWE graphs for each ICD code as the support set, and the query set has 15 HEWE graphs for each ICD code in every training episode. That is, $K = 5$ and $L = 15$ when trains CoGraph. In the testing stage, we use $C = 5$ and $K = 5$ for comparison. We initialize the parameters of CoGraph randomly and use a batch size of 64 in the few-shot learning stage. The Adam optimizer [19] is used to optimize the parameters of CoGraph and the maximum training epochs is set 300. The learning rate λ is 0.001 and the momentum parameters are set to the defaults

$\beta_1 = 0.9$ and $\beta_2 = 0.999$. We implement CoGraph in Pytorch and train it on a GeForce GTX TitanX GPU⁴.

6 RESULT

6.1 Performance on rare ICD codes

To assess the performance of CoGraph on rare ICD codes (i.e., codes that occur fewer than 10 times, and more than 2 times in the MIMIC-III data), we report the evaluation metrics for rare ICD codes in the left half of Table 2. Based on Table 2, we have several observations. First, CoGraph achieves the best performance on most of the evaluation metrics, such as ACC, Precision, Recall and F1. This indicates that CoGraph is able to effectively perform rare ICD classification by transferring knowledge between different ICD codes. Importantly, the F1 get an improvement of 2.95% over the best baseline, i.e., PrototypeNet-attention, and compared to the worst baseline, i.e., MLP, the improvement in F1 is 47.23%. The reason for these improvements is that CoGraph can transfer classification knowledge between different ICD codes, using our two graph contrastive learning schemes to capture the intra-graph and inter-graph correlations.

Second, on the classification of rare ICD codes, the few-shot learning based methods (i.e., MatchingNet, PrototypeNet, PrototypeNet-attention and RelationNet-attention) perform better than other methods (i.e., MLP, BI-GRU, CAML, DR-CAML and MSATT-KG). Among them, MLP and BI-GRU are relatively simple baselines and perform poorly, while CAML, DR-CAML and MSATT-KG all consider the description information of ICD codes, and have more powerful architectures, so compared to MLP and BI-GRU, they can get better results. Since the imbalance in the distribution of ICD codes and the lack of training samples are not considered by the non-few-shot learning methods, their performance is much worse than that of the few-shot learning based methods.

Third, the performance differences between different few-shot learning methods are small. For example, the F1 of Prototype-attention only improves by 0.13% over the MatchingNet. This is because these few-shot learning methods are all metric-based methods, and the differences between them are only in the similarity measurements of support set and query set. Thanks to its attention mechanism, the accuracy and precision of PrototypeNet-attention have been improved by 2.73% compared to PrototypeNet.

6.2 Performance on frequent ICD codes

To assess the performance of CoGraph on frequent ICD codes, we report the evaluation metrics for frequent ICD codes in the right half of Table 2. Based on Table 2, we have some observations. First, CoGraph achieves the best performance on most of the evaluation metrics, such as ACC, Recall and F1, but not Precision. This indicates

that CoGraph is able to effectively perform frequent ICD classification by episode-based meta-training on different ICD codes. The F1 gets a slight improvement of 0.61% over the best baseline, i.e., PrototypeNet-attention, and compared to the worst baseline, i.e., MLP, the increase in F1 is 54.90%. In addition, the recall values are significantly lower than precision values in most of the baselines and CoGraph, indicating that they tend to neglect some correct ICD codes.

Second, unlike on rare ICD codes, CAML, DR-CAML and MSATT-KG perform better than some few-shot learning-based methods, such as MatchingNet and PrototypeNet. These results indicate that CAML, DR-CAML and MSATT-KG methods are very effective if they are fed sufficiently many training samples, but they cannot obtain a good classification model when the training set contains only a few training samples.

Third, compared to frequent ICD codes, CoGraph has a bigger advantage over competing methods on rare ICD codes. For example, on the rare ICD codes, the F1 of CoGraph improves by 2.95% over the best baseline. On the frequent ICD codes, our CoGraph also gets a slight improvement, i.e., 0.61%, over the best baseline. The reason is that CoGraph is pre-trained by two effective graph-based contrastive learning schemes, i.e., GSCL and GECL, which prompt the CoGraph to learn graph features that are independent of the ICD codes. Furthermore, these independent graph features can be transferred to the ICD coding task in the few-shot learning stage.

7 ANALYSIS

7.1 Ablation study

We conduct an ablation study to analyze the effects of different components in CoGraph, as shown in Table 3. These are the variants of our method that we consider: 1) -GECL-GSCL denotes CoGraph without graph contrastive learning schemes. We remove the graph contrastive learning schemes and just use graph-based few-shot learning to train our model. 2) -GECL denotes CoGraph without GECL. 3) -GSCL denotes CoGraph without GSCL. From the results, we obtain the following insights:

First, the performance of CoGraph on both rare and frequent ICD codes decreases dramatically after removing graph evolution and graph sampling contrastive learning (i.e., -GECL-GSCL). Specifically, the F1 values drop by 7.27% and 6.12% on rare and frequent ICD codes, respectively. The result shows that using graph contrastive learning schemes to pre-train the graph encoder plays a crucial role in the few-shot learning stage. This is because GSCL and GSCL do not require the supervision of ICD codes, which helps to learn more general graph features. At the same time, GECL captures the inter-graph correlations by comparing graph sequences, while GSCL contrasts sub-graphs to obtain the intra-graph correlations between them. Both contrastive learning schemes can pre-train a more robust graph encoder. In the few-shot

4. The source code is available at <https://github.com/WOW5678/CoGraph>.

TABLE 2: Performance comparison (%) of different methods. **Bold face** indicates the best result in terms of the corresponding metric. Significant improvements over the best baseline results are marked with * (t-test, $p < 0.05$).

Method	Rare ICD codes				Frequent ICD codes			
	ACC	Precision	Recall	F1	ACC	Precision	Recall	F1
MLP	19.62	7.98	20.70	10.41	20.41	9.07	20.73	11.31
BI-GRU	20.91	8.06	21.76	11.14	36.04	36.29	38.37	35.55
CAML	23.56	16.44	17.80	16.86	63.02	69.94	62.11	63.78
DR-CAML	16.77	17.43	17.48	16.97	62.60	68.98	62.41	63.76
MSATT-KG	16.04	17.28	16.58	15.44	63.33	63.53	64.79	62.18
MatchingNet	54.95	60.17	54.90	54.56	61.56	68.22	61.89	61.23
PrototypeNet	52.21	61.34	51.54	51.96	61.04	67.09	59.70	60.97
PrototypeNet-attention	54.73	61.49	54.80	54.69	63.96	73.20	64.22	65.60
RelationNet-attention	52.92	55.75	53.11	53.02	61.88	68.79	61.94	62.71
CoGraph	57.07*	69.81	56.37	57.64*	65.27*	71.46	65.32*	66.21*

TABLE 3: Analysis of different components in CoGraph. **Bold face** indicates the best result in terms of the corresponding metric. Significant improvements over the best baseline results are marked with * (t-test, $p < 0.05$).

Method	Rare ICD codes				Frequent ICD codes			
	ACC	Precision	Recall	F1	ACC	Precision	Recall	F1
-GECL-GSCL	50.30	64.72	50.73	50.37	60.62	64.63	60.07	60.09
-GECL	55.90	69.16	56.15	56.36	62.71	71.64	65.91	65.27
-GSCL	56.05	69.00	55.92	56.61	63.02	68.72	61.78	63.30
CoGraph	57.07	69.81	56.37*	57.64	65.27	71.46	65.32	66.21*

learning stage, the graph encoder is fine-tuned to adapt to the classification of different ICD codes.

Second, compared to frequent ICD codes, the GSCL and GECL schemes have almost the same effect on rare ICD codes. When the GECL and GSCL schemes are removed, the model’s ACC and F1 decreases by 1.25% and 1.03% on rare ICD codes and by 0.94% and 2.91% on frequent ICD codes. That’s because the graph contrastive learning schemes do not require ICD labels. More specifically, GSCL and GECL prompt the CoGraph to learn features that do not rely on ICD labels. So compared to rare ICD codes, the pre-trained graph encoder plays almost the same role in the frequent ICD classification even though the data is unbalanced. These figures confirms that class-imbalanced learning can significantly benefit in self-supervised manners [56].

Third, after removing the GECL or GSCL module, the performance of CoGraph decreases on both rare ICD and frequent ICD. Specifically, on the rare ICD, the ACC of CoGraph drops from 57.07% to 55.90% (i.e., -GECL) and to 56.05% (i.e., -GSCL), while on the frequent ICD, the ACC of CoGraph drops by 2.56% and 2.25% respectively. This fully shows that the graph encoder pre-trained by GECL and GSCL has learned different aspects of the HEWE graph and that GECL and GSCL are helpful for the classification of rare and frequent ICD codes. This result is in line with our initial intuition: GECL learns correlations between graphs, while GSCL learns the intra-graph correlations. So it is effective for CoGraph to combine GECL and GSCL to learn graph structures.

7.2 Graph embedding visualization

In this section, we analyze the HEWE graph embeddings learned using two contrastive schemes to see if they learn any informative representations during the pre-training stage. We randomly select 5 ICD codes from

the test set, each of which contains 1000 samples, and use the t-Distributed Stochastic Neighbor Embedding (t-SNE) [47] for high-dimensional embedding exploration and visualizing. The results are shown in Fig. 5.

Comparing Fig. 5(d) with the other figures in terms of their densities of HEWE graph embeddings, we can see that graph embeddings with both GSCL and GECL can learn tighter clusters for the ICD codes. For example, most of the samples belonging to V10.46 are closely located to one another in Fig. 5(d). This indicates that pre-training the graph encoder by combining GSCL and GECL can obtain better representations of the HEWE graphs, compared with the other cases, i.e. without pre-training (Fig. 5(a)) or using a single graph contrastive learning scheme (Fig. 5(b) and Fig. 5(c)).

It is worth noting that although most of the samples belonging to the same ICD code are grouped together, the boundaries between different clusters are not obvious. We think that this is related to the goal of few-shot learning, which is to find out *the most similar support samples* for the query samples by maximizing the similarities between query and support samples [21], so as to conduct the ICD prediction for the query samples. It does not care about the mapping between the samples and the ICD codes. As a result, there are no clear boundaries among the different ICD clusters.

7.3 Impact of few-shot size

This work studies few-shot EHR coding, thus we conduct experiments to analyze the impact of the few-shot size K . Figure 6 reports the performance of CoGraph on rare and frequent ICD codes with different settings of K . First, with an increase in K , the performances of CoGraph on rare ICD codes shows an increase. Specifically, when K increases from 1 to 5, ACC, Precision, Recall, and F1 all

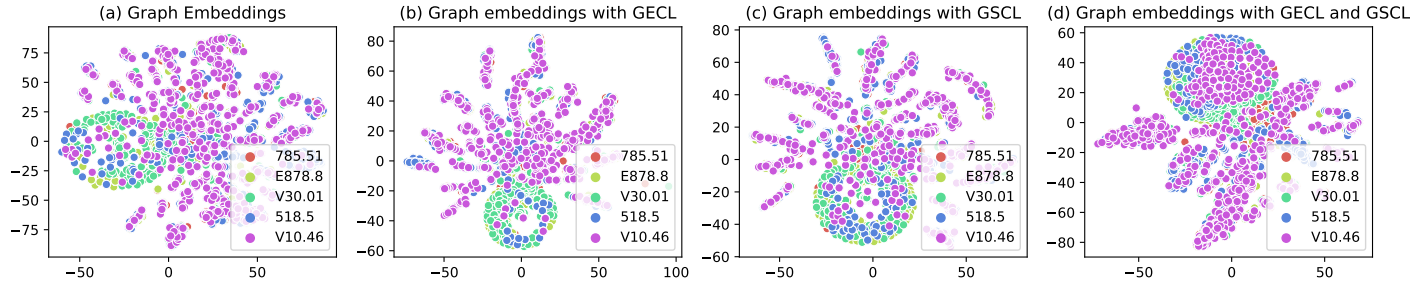


Fig. 5: Graph embedding with different pre-trained graph encoder.

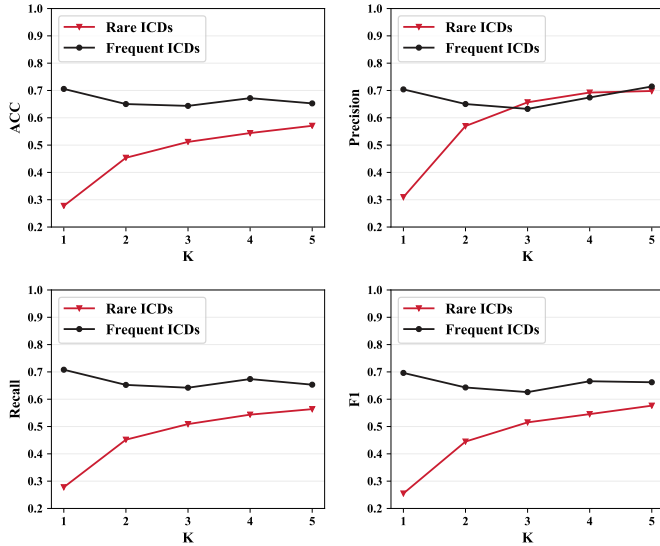


Fig. 6: Impact on the rare and frequent ICD codes of few-shot size K .

show an upward trend, in which the F1 increases from 25.48% to 57.64%. This indicates that a larger support set can produce better prediction results of the rare ICD codes. A larger support set can provide more supervision information for query HEWE graphs from rare ICD codes, which is conducive to the classification of query samples [6].

Second, when the support size K increases from 1 to 2, the performance of CoGraph has the greatest improvement. For example, when K increases from 1 to 4, the F1 increases by 19.01%, 6.72%, 3.33%. Further, when K increases from 4 to 5, the F1 value increases by 3.10%. So this upward trend of model’s performance on rare ICD codes becomes lightly gradually with the increase of K . When K is very small, the main factor limiting the model’s performance on rare ICD codes is the lack of supervision information. However, with the continuous increase of K , the lack of supervision information is no longer its biggest limitation [41]. Therefore, ACC, Precision, Recall, and F1 tend to increase slower as K increases.

Third, the performance of CoGraph on frequent ICD codes does not increase with the increase of K , but has a slight downward trend. Specifically, when K increases from 1 to 3, the F1 value of CoGraph gradually decreases by 5.33% and 1.70% respectively. As K continues to increase, the performance of CoGraph begins to fluctuate slightly. In short, CoGraph has the best performance on

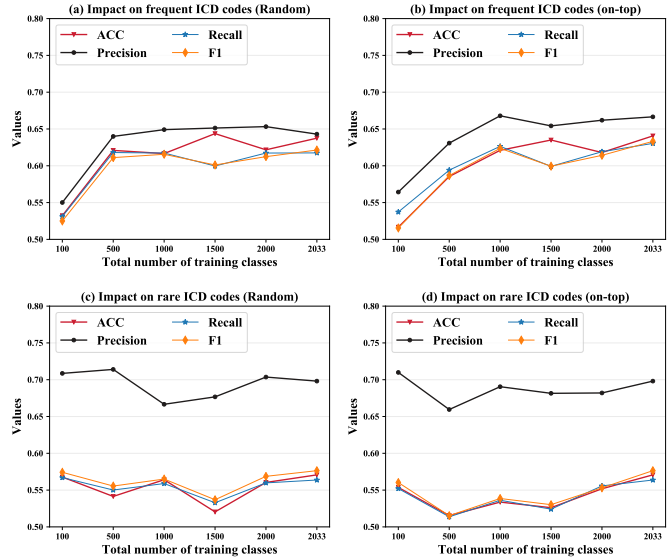


Fig. 7: Impact of varying number of training classes with different sampling modes.

frequent ICD codes when K is 1. When K is 1, there is very little supervision information for the rare ICD codes, which makes the model pay more attention to the classification of frequent ICD codes. As K increases, the supervision information of rare ICD codes prompts CoGraph to learn features that can be generalized to the rare ICD classification, so the classification performance of CoGraph on frequent ICD codes has slightly decreased.

7.4 Impact of training ICD classes

CoGraph iteratively samples C -way different ICD classes for training, and the remaining ICD classes are as the support set and query set. Suggested by [24], we conduct an analysis experiment to analyze the effect of the sampling strategies as well as the number of ICD classes on the performance, and the results are shown in Fig 7.

Fig 7 (a) and (b) illustrate the changing trends of CoGraph’s performance on frequent ICD codes with different sampling strategies, i.e., “random” and “on-top”. The former selects the ICD classes for training randomly, while the latter selects in descending order by the number of samples in each class. It can be seen that no matter which sampling strategy is used, the performances of CoGraph on frequent ICD codes rise first and then stabilize. CoGraph fluctuates more with the “on-top” strategy relatively. We believe that the main reason is that the “on-top” strategy is an uneven sampling strategy where

ICD codes with a large number of samples are easy to dominate, leading to unstable learning eventually.

Fig 7 (c) and (d) illustrate the changing trends of CoGraph's performance on rare ICD codes with "random" and "on-top" sampling strategies. We can observe that the overall performance of CoGraph remains stable with slight fluctuations, which indicates that the increase of the training classes has little influence on the performance of CoGraph in terms of the rare ICD codes. This means that CoGraph trained with 100 ICD codes already has sufficient learning and transfer the necessary knowledge from frequent ICD codes to rare ICD codes. In addition, the Precision values of CoGraph are significantly higher than Recall and ACC values for the rare ICD codes. This is because that the extremely rare ICD codes are easy to be neglected, indicating that there is still room for further improvement on the extremely rare ICD codes.

8 CONCLUSION

In this work, we reformulate electronic health record (EHR) coding as a few-shot learning task, and propose a graph-based few-shot learning framework, i.e., CoGraph, to perform ICD classification on both frequent and rare ICD codes. As part of CoGraph, we design two graph contrastive learning schemes, i.e., GSCL and GSC, to pre-train the graph encoder in the few-shot learning framework. GSCL captures the intra-correlations within the graphs by comparing the structured features of sub-graphs, while GECL captures the inter-correlations between the graphs at different clinical stages by comparing the historical graph sequence and the future graph.

A limitation of CoGraph is that it only extracts the high-frequency words and entities from free-text of EHRs; it does not take medical knowledge or rules into account. However, medical knowledge or rules may help to perform ICD classification, such as the concurrency and hierarchy of some ICD codes. As to future work, we plan to model the correlations of ICD codes to learn better transferable features. Then, we hope to further improve the classification performances of CoGraph, especially on the rare ICD codes.

ACKNOWLEDGEMENTS

This research was partially supported by the Natural Science Foundation of China (61972234, 61902219, 62072279), the National Key R&D Program of China with grant No. 2020YFB1406704, the Key Scientific and Technological Innovation Program of Shandong Province (2019JZZY010129), the Tencent WeChat Rhino-Bird Focused Research Program (JR-WXG-2021411), the Fundamental Research Funds of Shandong University, and the Hybrid Intelligence Center, a 10-year programme funded by the Dutch Ministry of Education, Culture and Science through the Netherlands Organisation for Scientific Research, <https://hybrid-intelligence-centre.nl>. All content represents the opinion of the authors, which

is not necessarily shared or endorsed by their respective employers and/or sponsors.

REFERENCES

- [1] Anand Avati, Kenneth Jung, Stephanie Harman, Lance Downing, Andrew Y. Ng, and Nigam H. Shah. Improving palliative care with deep learning. In *IEEE International Conference on Bioinformatics and Biomedicine*, pages 311–316, 2017.
- [2] Tal Baumel, Jumana Nassour-Kassis, Raphael Cohen, Michael Elhadad, and Noémie Elhadad. Multi-label classification of patient notes: Case study on ICD code assignment. In *The Workshops of the The Thirty-Second AAAI Conference on Artificial Intelligence*, pages 409–416, 2018.
- [3] Ting Chen, Yizhou Sun, Yue Shi, and Liangjie Hong. On sampling strategies for neural network-based collaborative filtering. In *Proceedings of the 23rd ACM SIGKDD International Conference on Knowledge Discovery and Data Mining*, pages 767–776, 2017.
- [4] Ting Chen, Simon Kornblith, Mohammad Norouzi, and Geoffrey E. Hinton. A simple framework for contrastive learning of visual representations. In *Proceedings of the 37th International Conference on Machine Learning*, pages 1597–1607, 2020.
- [5] Edward Choi, Mohammad Taha Bahadori, Andy Schuetz, Walter F. Stewart, and Jimeng Sun. Doctor AI: predicting clinical events via recurrent neural networks. In *Proceedings of the 1st Machine Learning in Health Care*, pages 301–318, 2016.
- [6] Kaize Ding, Jianling Wang, Jundong Li, Kai Shu, Chenghao Liu, and Huan Liu. Graph prototypical networks for few-shot learning on attributed networks. In *The 29th ACM International Conference on Information and Knowledge Management*, pages 295–304, 2020.
- [7] Chelsea Finn, Pieter Abbeel, and Sergey Levine. Model-agnostic meta-learning for fast adaptation of deep networks. In *Proceedings of the 34th International Conference on Machine Learning*, pages 1126–1135, 2017.
- [8] Akira Fukui, Dong Huk Park, Daylen Yang, Anna Rohrbach, Trevor Darrell, and Marcus Rohrbach. Multimodal compact bilinear pooling for visual question answering and visual grounding. In *Proceedings of the 2016 Conference on Empirical Methods in Natural Language Processing*, pages 457–468, 2016.
- [9] Tianyu Gao, Xingcheng Yao, and Danqi Chen. Simcse: Simple contrastive learning of sentence embeddings. *CoRR*, abs/2104.08821, 2021.
- [10] Ruiying Geng, Binhua Li, Yongbin Li, Jian Sun, and Xiaodan Zhu. Dynamic memory induction networks for few-shot text classification. In *Proceedings of the 58th Annual Meeting of the Association for Computational Linguistics*, pages 1087–1094, 2020.
- [11] Cyril Goutte and Eric Gaussier. A probabilistic interpretation of precision, recall and f-score, with

- implication for evaluation. In *European Conference on Information Retrieval*, pages 345–359, 2005.
- [12] Kaiming He, Haoqi Fan, Yuxin Wu, Saining Xie, and Ross B. Girshick. Momentum contrast for unsupervised visual representation learning. In *IEEE/CVF Conference on Computer Vision and Pattern Recognition*, pages 9726–9735, 2020.
- [13] Jin Huang and Charles X Ling. Using auc and accuracy in evaluating learning algorithms. *IEEE Transactions on knowledge and Data Engineering*, 17(3): 299–310, 2005.
- [14] Jinmiao Huang, Cesar Osorio, and Luke Wicent Sy. An empirical evaluation of deep learning for ICD-9 code assignment using MIMIC-III clinical notes. *Computer Methods and Programs in Biomedicine*, 177: 141–153, 2019.
- [15] Glen Jeh and Jennifer Widom. Scaling personalized web search. In *Proceedings of the Twelfth International World Wide Web Conference*, pages 271–279, 2003.
- [16] Yizhu Jiao, Yun Xiong, Jiawei Zhang, Yao Zhang, Tianqi Zhang, and Yangyong Zhu. Sub-graph contrast for scalable self-supervised graph representation learning. *arXiv preprint arXiv:2009.10273*, 2020.
- [17] Alistair EW Johnson, Tom J Pollard, Lu Shen, H Lehman Li-Wei, Mengling Feng, Mohammad Ghassemi, Benjamin Moody, Peter Szolovits, Leo Anthony Celi, and Roger G Mark. MIMIC-III, a freely accessible critical care database. *Scientific data*, 3(1):1–9, 2016.
- [18] Yoon Kim. Convolutional neural networks for sentence classification. In *Proceedings of Conference on Empirical Methods in Natural Language Processing*, pages 1746–1751, 2014.
- [19] Diederik P. Kingma and Jimmy Ba. Adam: A method for stochastic optimization. In *3rd International Conference on Learning Representations*, 2015.
- [20] Thomas N. Kipf and Max Welling. Semi-supervised classification with graph convolutional networks. In *5th International Conference on Learning Representations*, 2017.
- [21] Yu Li, Lei Zhang, Wei Wei, and Yanning Zhang. Deep self-supervised learning for few-shot hyperspectral image classification. In *IEEE International Geoscience and Remote Sensing Symposium*, pages 501–504, 2020.
- [22] Zhenguo Li, Fengwei Zhou, Fei Chen, and Hang Li. Meta-sgd: Learning to learn quickly for few shot learning. *CoRR*, abs/1707.09835, 2017.
- [23] Andrea Madotto, Zhaojiang Lin, Chien-Sheng Wu, and Pascale Fung. Personalizing dialogue agents via meta-learning. In *Proceedings of the 57th Conference of the Association for Computational Linguistics*, pages 5454–5459, 2019.
- [24] Carlos Medina, Arnout Devos, and Matthias Grossglauser. Self-supervised prototypical transfer learning for few-shot classification. *CoRR*, abs/2006.11325, 2020.
- [25] Tomas Mikolov, Ilya Sutskever, Kai Chen, Greg S Corrado, and Jeff Dean. Distributed representations of words and phrases and their compositionality. In *Advances in Neural Information Processing Systems*, volume 26, pages 3111–3119, 2013.
- [26] Nikhil Mishra, Mostafa Rohaninejad, Xi Chen, and Pieter Abbeel. A simple neural attentive meta-learner. In *6th International Conference on Learning Representations*, 2018.
- [27] James Mullenbach, Sarah Wiegrefe, Jon Duke, Jimeng Sun, and Jacob Eisenstein. Explainable prediction of medical codes from clinical text. In *Proceedings of the 2018 Conference of the North American Chapter of the Association for Computational Linguistics: Human Language Technologies*, pages 1101–1111, 2018.
- [28] James Mullenbach, Sarah Wiegrefe, Jon Duke, Jimeng Sun, and Jacob Eisenstein. Explainable prediction of medical codes from clinical text. In *Proceedings of the 2018 Conference of the North American Chapter of the Association for Computational Linguistics: Human Language Technologies*, pages 1101–1111, 2018.
- [29] Zhen Peng, Yixiang Dong, Minnan Luo, Xiao-Ming Wu, and Qinghua Zheng. Self-supervised graph representation learning via global context prediction. *CoRR*, abs/2003.01604, 2020.
- [30] Aaditya Prakash, Siyuan Zhao, Sadid A. Hasan, Vivek V. Datla, Kathy Lee, Ashequl Qadir, Joey Liu, and Oladimeji Farri. Condensed memory networks for clinical diagnostic inferencing. In *Proceedings of the Thirty-First Conference on Artificial Intelligence*, pages 3274–3280, 2017.
- [31] Tiexin Qin, Wenbin Li, Yinghuan Shi, and Yang Gao. Unsupervised few-shot learning via distribution shift-based augmentation. *CoRR*, abs/2004.05805, 2020.
- [32] Jiezhong Qiu, Qibin Chen, Yuxiao Dong, Jing Zhang, Hongxia Yang, Ming Ding, Kuansan Wang, and Jie Tang. GCC: graph contrastive coding for graph neural network pre-training. In *The 26th ACM SIGKDD Conference on Knowledge Discovery and Data Mining*, pages 1150–1160, 2020.
- [33] Sachin Ravi and Hugo Larochelle. Optimization as a model for few-shot learning. In *5th International Conference on Learning Representations*, 2017.
- [34] Vivek Roy, Yan Xu, Yu-Xiong Wang, Kris Kitani, Ruslan Salakhutdinov, and Martial Hebert. Few-shot learning with intra-class knowledge transfer. *CoRR*, abs/2008.09892, 2020.
- [35] Othman Sbai, Camille Couprie, and Mathieu Aubry. Impact of base dataset design on few-shot image classification. In *Computer Vision - 16th European Conference*, pages 597–613, 2020.
- [36] Haoran Shi, Pengtao Xie, Zhiting Hu, Ming Zhang, and Eric P. Xing. Towards automated ICD coding using deep learning. *CoRR*, abs/1711.04075, 2017.
- [37] Jake Snell, Kevin Swersky, and Richard Zemel. Prototypical networks for few-shot learning. In *Advances in neural information processing systems*, pages 4077–4087, 2017.

- [38] Jake Snell, Kevin Swersky, and Richard S. Zemel. Prototypical networks for few-shot learning. In *Annual Conference on Neural Information Processing Systems*, pages 4077–4087, 2017.
- [39] Kihyuk Sohn. Improved deep metric learning with multi-class n-pair loss objective. In *Annual Conference on Neural Information Processing Systems*, pages 1849–1857, 2016.
- [40] Jong-Chyi Su, Subhransu Maji, and Bharath Hariharan. When does self-supervision improve few-shot learning? *CoRR*, abs/1910.03560, 2019.
- [41] Jong-Chyi Su, Subhransu Maji, and Bharath Hariharan. When does self-supervision improve few-shot learning? In *Computer Vision - 16th European Conference*, pages 645–666, 2020.
- [42] Flood Sung, Yongxin Yang, Li Zhang, Tao Xiang, Philip H. S. Torr, and Timothy M. Hospedales. Learning to compare: Relation network for few-shot learning. In *IEEE Conference on Computer Vision and Pattern Recognition*, pages 1199–1208, 2018.
- [43] Flood Sung, Yongxin Yang, Li Zhang, Tao Xiang, Philip HS Torr, and Timothy M Hospedales. Learning to compare: Relation network for few-shot learning. In *Proceedings of the IEEE Conference on Computer Vision and Pattern Recognition*, pages 1199–1208, 2018.
- [44] Fei Teng, Wei Yang, Li Chen, LuFei Huang, and Qiang Xu. Explainable prediction of medical codes with knowledge graphs. *Frontiers in Bioengineering and Biotechnology*, 8:867, 2020.
- [45] Yonglong Tian, Dilip Krishnan, and Phillip Isola. Contrastive multiview coding. *CoRR*, abs/1906.05849, 2019.
- [46] Aäron van den Oord, Yazhe Li, and Oriol Vinyals. Representation learning with contrastive predictive coding. *CoRR*, abs/1807.03748, 2018.
- [47] Laurens van der Maaten and Geoffrey Hinton. Visualizing data using t-sne. *Journal of Machine Learning Research*, 9(86):2579–2605, 2008.
- [48] Petar Velickovic, William Fedus, William L. Hamilton, Pietro Liò, Yoshua Bengio, and R. Devon Hjelm. Deep graph infomax. In *7th International Conference on Learning Representations*, 2019.
- [49] Oriol Vinyals, Charles Blundell, Tim Lillicrap, Koray Kavukcuoglu, and Daan Wierstra. Matching networks for one shot learning. In *Annual Conference on Neural Information Processing Systems*, pages 3630–3638, 2016.
- [50] Sen Wang, Xiaojun Chang, Xue Li, Guodong Long, Lina Yao, and Quan Z. Sheng. Diagnosis code assignment using sparsity-based disease correlation embedding. *IEEE Transactions on Knowledge and Data Engineering*, 28(12):3191–3202, 2016.
- [51] Shanshan Wang, Pengjie Ren, Zhumin Chen, Zhaochun Ren, Jun Ma, and Maarten de Rijke. Order-free medicine combination prediction with graph convolutional reinforcement learning. In *Proceedings of the 28th ACM International Conference on Information and Knowledge Management*, page 1623–1632, 2019.
- [52] Shanshan Wang, Pengjie Ren, Zhumin Chen, Zhaochun Ren, Jian-Yun Nie, Jun Ma, and Maarten de Rijke. Coding electronic health records with adversarial reinforcement path generation. In *43rd international ACM SIGIR conference on Research and Development in Information Retrieval*, pages 801–810, 2020.
- [53] Zhirong Wu, Yuanjun Xiong, Stella X. Yu, and Dahua Lin. Unsupervised feature learning via non-parametric instance discrimination. In *IEEE Conference on Computer Vision and Pattern Recognition*, pages 3733–3742, 2018.
- [54] Xiancheng Xie, Yun Xiong, Philip S. Yu, and Yangyong Zhu. Ehr coding with multi-scale feature attention and structured knowledge graph propagation. In *Proceedings of the 28th ACM International Conference on Information and Knowledge Management*, pages 649–658, 2019.
- [55] Keyang Xu, Mike Lam, Jingzhi Pang, Xin Gao, Charlotte Band, Piyush Mathur, Frank Papay, Ashish K. Khanna, Jacek B. Cywinski, Kamal Maheshwari, Pengtao Xie, and Eric P. Xing. Multimodal machine learning for automated ICD coding. In *Proceedings of the Machine Learning for Healthcare Conference*, pages 197–215, 2019.
- [56] Yuzhe Yang and Zhi Xu. Rethinking the value of labels for improving class-imbalanced learning. In *Advances in Neural Information Processing Systems*, volume 33, pages 19290–19301, 2020.
- [57] Mang Ye, Xu Zhang, Pong C. Yuen, and Shih-Fu Chang. Unsupervised embedding learning via invariant and spreading instance feature. In *IEEE Conference on Computer Vision and Pattern Recognition*, pages 6210–6219, 2019.
- [58] Qing Yu, Hui Zhao, and Zuohua Wang. Attention-based bidirectional gated recurrent unit neural networks for sentiment analysis. In *Proceedings of the 2nd International Conference on Artificial Intelligence and Pattern Recognition*, pages 116–119, 2019.
- [59] Jiaqi Zeng and Pengtao Xie. Contrastive self-supervised learning for graph classification. *CoRR*, abs/2009.05923, 2020.
- [60] Danchen Zhang, Daqing He, Sanqiang Zhao, and Lei Li. Enhancing automatic ICD-9-CM code assignment for medical texts with pubmed. In *Workshop on Biomedical Natural Language Processing*, pages 263–271, 2017.
- [61] Jiawei Zhang, Haopeng Zhang, Congying Xia, and Li Sun. Graph-bert: Only attention is needed for learning graph representations. *CoRR*, abs/2001.05140, 2020.
- [62] Peng Zhou, Wei Shi, Jun Tian, Zhenyu Qi, Bingchen Li, Hongwei Hao, and Bo Xu. Attention-based bidirectional long short-term memory networks for relation classification. In *Proceedings of the 54th Annual Meeting of the Association for Computational Linguistics*, pages 207–212, 2016.